Validating Wind-Induced Response of Tall Buildings: Synopsis of the Chicago Full-Scale Monitoring Program

Tracy Kijewski-Correa, M.ASCE[1]; John Kilpatrick[2]; Ahsan Kareem, M.ASCE[3]; Dae-Kun Kwon[4]; Rachel Bashor, S.M.ASCE[5]; Michael Kochly, S.M.ASCE[6]; Bradley S. Young, M.ASCE[7]; Ahmad Abdelrazaq, M.ASCE[8]; Jon Galsworthy, M.ASCE[9]; Nicholas Isyumov, F.ASCE[10]; Dave Morrish[11]; Robert C. Sinn, F.ASCE[12]; and William F. Baker, F.ASCE[13]

Abstract: Tall buildings are one of the few constructed facilities whose design relies solely upon analytical and scaled models, which, though based upon fundamental mechanics and years of research and experience, has yet to be systematically validated in full scale. In response to this need, through the combined efforts of members of academe, a design firm and a commercial wind tunnel testing laboratory, a program was initiated to monitor the full-scale response of representative tall buildings and compare this to the predicted response from wind tunnels and finite-element models used commonly in design. As part of this monitoring program, in situ periods and damping ratios over a range of response amplitudes are also being evaluated. This paper provides an overview of the monitoring program, which includes three tall buildings in the city of Chicago, details their instrumentation and modeling, and provides an example of the full-scale response data analyses being conducted.

DOI: 10.1061/(ASCE)0733-9445(2006)132:10(1509)

CE Database subject headings: Wind forces; Dynamic response; Wind tunnels; Damping; Global positioning; Buildings, high-rise; Illinois; Chicago.

Introduction

Even though the performance of tall buildings affects the safety and comfort of a large number of people in both residential and office environments, tall buildings are one of the few constructed facilities whose design relies solely upon analytical and scaled models, which, though based upon fundamental mechanics and years of research and experience, has yet to be systematically validated in full scale. In particular, as state-of-the-art structural analysis software and wind tunnel testing are advancing rapidly, the accuracy and validity of their results needs to be calibrated with respect to actual performance. Understandably, since the development of full-scale models for this type of structure is not feasible, monitoring the performance of actual structures becomes the most viable means for verification and improvement of current design practices and analytical modeling approaches. The latter becomes particularly important to ensure satisfactory performance, economy, and efficiency of future designs of increased complexity and height.

Limiting motion perception by building occupants is often a

[1]Rooney Family Assistant Professor, Univ. of Notre Dame, 156 Fitzpatrick Hall, Notre Dame, IN 46556 (corresponding author). E-mail: tkijewsk@nd.edu

[2]Graduate Student, The Boundary Layer Wind Tunnel, Faculty of Engineering, The Univ. of Western Ontario, London ON, Canada N6A 5B9. E-mail: jkilpatr@uwo.ca

[3]Robert M. Moran Professor, Univ. of Notre Dame, 156 Fitzpatrick Hall, Notre Dame, IN 46556. E-mail: kareem@nd.edu

[4]Postdoctoral Research Associate, Univ. of Notre Dame, 156 Fitzpatrick Hall, Notre Dame, IN 46556. E-mail: daekun.kwon.4@nd.edu

[5]Graduate Student, Univ. of Notre Dame, 156 Fitzpatrick Hall, Notre Dame, IN 46556. E-mail: rstansel@nd.edu

[6]Graduate Student, Univ. of Notre Dame, 156 Fitzpatrick Hall, Notre Dame, IN 46556. E-mail: mkochly@nd.edu

[7]Engineer, Skidmore, Owings & Merrill LLP, Suite 1000, 224 South Michigan Ave., Chicago, IL 60604. E-mail: bradley.young@som.com

[8]Vice President/Executive Director, Architectural Design and Engineering Consulting Division, Samsung Corporation, Samsung Engineering and Construction Group, 12th Floor, Samsung Plaza, 263, Seohyun-Dong, Bundang-Gu, Sungnam-Si, Gyonggi-Do, Korea 463-721. E-mail: ahmad.abdelrazaq1@samsung.com

[9]Associate Research Director, The Boundary Layer Wind Tunnel, Faculty of Engineering, The Univ. of Western Ontario, London ON, Canada N6A 5B9. E-mail: jg@blwtl.uwo.ca

[10]Research Consultant, The Boundary Layer Wind Tunnel, Faculty of Engineering, The Univ. of Western Ontario, London ON, Canada, N6A 5B9. E-mail: ni@blwtl.uwo.ca

[11]Manager of Information and Measurement Technology, The Boundary Layer Wind Tunnel, Faculty of Engineering, The Univ. of Western Ontario, London ON, Canada N6A 5B9. E-mail: dpm@blwtl.uwo.ca

[12]Associate Partner, Skidmore, Owings & Merrill LLP, Suite 1000, 224 South Michigan Ave., Chicago, IL 60604. E-mail: robert.c.sinn@som.com

[13]Partner, Skidmore, Owings & Merrill LLP, Suite 1000, 224 South Michigan Ave., Chicago, IL 60604. E-mail: william.baker@som.com

Note. Associate Editor: Kurtis R. Gurley. Discussion open until March 1, 2007. Separate discussions must be submitted for individual papers. To extend the closing date by one month, a written request must be filed with the ASCE Managing Editor. The manuscript for this paper was submitted for review and possible publication on April 1, 2005; approved on December 8, 2005. This paper is part of the ***Journal of Structural Engineering***, Vol. 132, No. 10, October 1, 2006. ©ASCE, ISSN 0733-9445/2006/10-1509–1523/$25.00.

Table 1. General Structural Properties of Monitored Buildings

Building	Material	System	Occupancy	Density	Floor-to-floor height
1	Steel	Tube	Office/residential	144.2 kg/m^3 (9.0 lb/ft^3)	2.7–3.8 m (9 ft 0 in.–12 ft 6 in.)
2	Concrete	Shear wall/outrigger	Office	288.3 kg/m^3 (18.0 lb/ft^3)	4.0 m (13 ft 0 in.)
3	Steel	Tube	Office	157.0 kg/m^3 (9.8 lb/ft^3)	3.9 m (12 ft 10 in.)

controlling structural engineering design parameter for tall buildings, even in moderate wind climates. Significant premium for height in terms of additional structural material may become necessary in order to satisfy current acceleration-based motion criteria that have been developed by researchers and practitioners in the last few decades. This premium is beyond that required to meet minimum standards for building strength or lateral drift serviceability criteria related to building partitions or other architectural systems such as cladding and facades. These accelerations can be reduced through aerodynamic shaping of the overall building form to directly reduce wind loads or by modifying either one or a combination of mass, stiffness or damping (e.g., Kareem et al. 1999). Increased damping has a demonstrated effectiveness in reducing motion in all situations. This may be accomplished qualitatively by a choice of material or structural system or quantitatively by supplemental devices. Increasing the mass and/or stiffness of a building reduces wind-induced accelerations in most situations. However, there can be exceptions and detailed information on the building response is necessary in order to ascertain their effects. Of the basic structural variables, only mass and stiffness are known with a reasonably high level of certainty in design. Damping, on the other hand, is a much more approximate building characteristic, which depends on a number of factors including structural materials, type of structural system and resulting force distribution, contributions of interior partitions and exterior cladding, and other nonstructural inputs. Although there have been some efforts to develop empirical predictive tools for damping estimation based on full-scale observations (Jeary 1986; Satake et al. 2003), there is still significant scatter in the data, as well as limited information for high rise buildings dominated by resonant response, though recently, efforts in The People's Republic of China, including Hong Kong, have added two significantly tall buildings to the full-scale damping literature (Li et al. 1998, 2002). Still, as the estimated damping design values have a coefficient of variation of up to 70%, there may be significant uncertainty in the resulting response quantities (Kareem and Gurley 1996), which are vital to ensure that the design satisfies occupant comfort criteria.

Full-scale monitoring provides the opportunity to directly correlate actual building performance, quantified in terms of lateral and torsional accelerations, to occupant perception criteria. Such efforts may lead to a more refined definition of criteria strongly impacting structural design of tall buildings. More importantly, full-scale measurements allow the validation of other modeling and design assumptions and expand existing databases of damping levels. Unfortunately, only limited studies have pursued full-scale investigations related to perception (Ohkuma et al. 1991; Ohkuma 1996; Denoon et al. 1999) and full-scale validations (Littler 1991; Li et al. 2004). Meanwhile, most published full-scale damping observations are derived from midrise buildings, associated largely with the recent Japanese database (Satake et al. 2003). In response to this need, a partnership between the University of Notre Dame (UND), the Boundary Layer Wind Tunnel Laboratory (BLWTL) at the University of Western Ontario (UWO) and Skidmore, Owings & Merrill LLP (SOM) in Chicago was established to initiate the Chicago full-scale monitoring program. Through the program, the actual performance of three tall buildings in Chicago is compared to predictions, both by finite-element and wind tunnel models, thereby providing an important missing link between analytical modeling and actual behavior. Based on these comparisons, the sources of discrepancies are identified to allow enhancement of current design practice. These evaluations also examine the in situ periods and damping ratios of the buildings under a variety of wind conditions and over a range of response amplitudes. As such, these efforts will enhance existing databases presently lacking substantial information on buildings of significant height and will provide important information on the variation of dynamic properties with amplitude.

Description of Instrumented Buildings

The primary objective of this study is to correlate the in-situ measured response characteristics of tall buildings in full scale, with computer-based analytical and wind tunnel models for the advancement of the current state-of-the-art in tall building design. Such an endeavor requires the selection of several buildings representative of structural systems common to high rise design, all located in the same general locale of downtown Chicago, for which design information and building access are obtainable. Since major effort was expended to establish relationships with the building owners to allow access, the anonymity of the buildings must be assured to guarantee continued access for the life of the program. Note that the reluctance of building owners to permit access to their buildings for instrumentation and monitoring has precluded earlier efforts from being realized not only in the United States but also abroad. As such, the structures will be genetically referenced as Buildings 1, 2, and 3. Each building utilizes straight shaft reinforced concrete caissons extending to bedrock. A brief description of noteworthy features of each building's structural system is now provided, with additional structural details summarized in Table 1.

Building 1

The primary lateral load-resisting system features a steel tube comprised of exterior columns, spandrel ties, and additional stiffening elements to achieve a near uniform distribution of load on the columns across the flange face, with very little shear lag. As such, lateral loads are resisted primarily by cantilever action, with the remainder carried by frame action.

Building 2

In this reinforced concrete building, shear walls located near the core of the building provide lateral load resistance. At two levels,

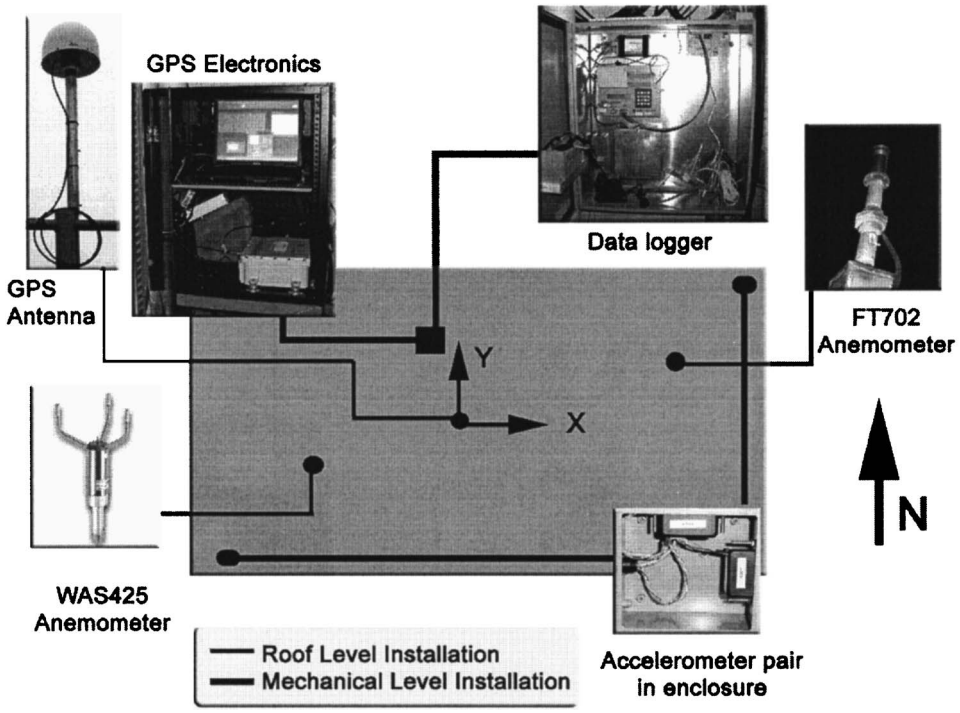

Fig. 1. Generalized sensor array on generic floor plan with inset photographs of equipment

this core is tied to the perimeter columns via reinforced concrete outrigger walls to control the wind drift and reduce overturning moment in the core shear walls.

Building 3

The steel moment-connected, framed tubular system of Building 3 behaves fundamentally as a vertical cantilever fixed at the base to resist wind loads. The system is comprised of closely spaced, wide columns and deep spandrel beams along multiple frame lines. Deformations of the structure are due to a combination of axial shortening, shearing, and flexure in the frame members, and beam–column panel zone distortions.

Dynamic Properties

In terms of dynamic characteristics, all three buildings have significant separation between their torsional and translational frequencies, being relatively stiff torsionally. As a result of this feature and other attributes, low torsional responses are expected. In light of their unique structural systems and the characteristics listed in Table 1, some hypotheses on inherent damping can also be made. Given that Building 1 has the lightest density and mostly axial deformations due to cantilever action, it is anticipated to have the lowest damping of the three buildings. Building 3, having similar density but comparatively larger contributions of flexure, shear, and panel zone effects to its overall deformation mechanism, is expected to have relatively higher damping. On the other hand, Building 2 is expected to have higher damping than either of its counterparts by virtue of its concrete construction. Finally, as each building is rectangular in plan, with the primary axes aligning with North and East, subsequent discussions will reference sway response as North-South (*N-S*) or *y* sway and East-West (*E-W*) or *x* sway for simplicity, as shown in Fig. 1.

Instrumentation Overview

Each building is equipped with the same primary instrumentation system that features four Columbia SA-107 LN high-sensitivity force-balance accelerometers, capable of accurately measuring accelerations down to 0 Hz, making them well suited for monitoring these long-period structures. A sensitivity of 15 V/g was selected for this study. These accelerometers are mounted in orthogonal pairs at two opposite corners of the ceiling at the highest possible floor in each building, as shown in Fig. 1. The outputs of these sensors are sampled every 0.12 s and archived by a 15-bit Campbell CR23X data logger. Considering the sensitivity of the accelerometers, the overall system resolution is approximately 0.001 milli-g. The logger is programmed to continuously capture 10-min statistics of these accelerometer outputs (min, max, and RMS), and when motions exceed a user-selected threshold, the system switches its acquisition mode to capture hour-long time histories for as long as the threshold levels are exceeded. The algebraic sum and difference of these four accelerometer outputs yield estimates of the *N-S* (*y*) and *E-W* (*x*) sway responses and provide two sources for estimation of the torsional response, respectively. The primary instrumentation systems were respectively installed in Buildings 1, 2, and 3 on June 14, 2002, June 15, 2002, and April 30, 2003.

While wind speed and direction are monitored regularly at Chicago's surrounding airports, since wind-induced accelerations are typically proportional to the wind velocity cubed, uncertainties in wind speed are very much amplified in the calculated building response. Thus, it becomes essential to have a reliable measure of wind speed and direction in the downtown area. Two ultrasonic anemometers were installed on masts 41 m above the rooftop of the tallest building in the program, Building 3, so that the reference wind speed and direction for each event may be

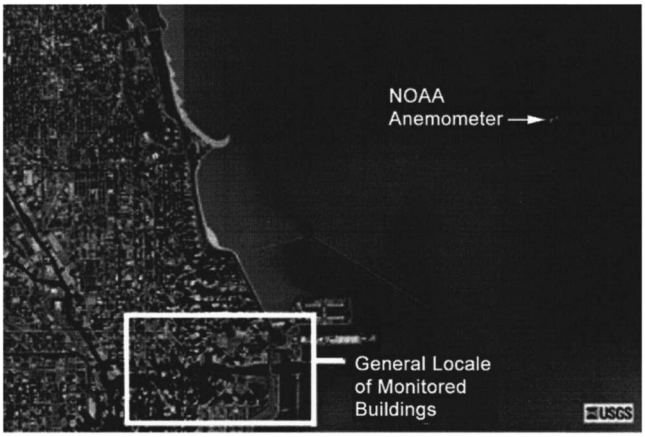

Fig. 2. Aerial photo of Chicago, Ill. (courtesy of USGS)

measured at this site and reliably converted to represent the wind speed at the top of each instrumented building. This installation was completed in the summer of 2004. The anemometers employed are the Vaisala WAS425 and FT Technologies FT702 ultrasonic anemometers with operating ranges of 0–65 and 0–70 m/s, respectively. Both units have resolutions of 0.1 m/s in wind speed and 1° in wind direction. The technical specifications of both anemometers were verified through wind speed and direction calibrations performed in the high speed wind tunnel at the BLWTL. These anemometers are at a record height in an urban zone posing unique challenges which include seasonal weather extremes, exposure to severe thunderstorms, immersion in dense rf environments, and potential rooftop interferences. In light of these challenges, the reliability of the measured data is presently being established utilizing wind information at different locations in the downtown area and wind tunnel tests.

An *interim wind monitoring protocol* was established in June 2002, while the final installation of these anemometers was coordinated at Building 3. This protocol continues to serve the program as the reliability of the rooftop anemometers is being assessed. This interim data is collected at the city's two airports (Midway and O'Hare) and from a NOAA GLERL meteorological station in Lake Michigan, elevated 23 m (~75 ft) above lake level and located 4.8 km (~3 mi) offshore of downtown Chicago (Fig. 2). The anemometer at this station is a Young 5103V, propeller-type sensor. Gradient wind speeds are estimated from the surface wind speeds measured at this NOAA met station. These data are extrapolated to gradient (taken as 300 m over open water) using methods to account for the influence of terrain roughness and fetch (ESDU 2001). A minor correction to the wind azimuth is also applied to account for the rotation of the velocity vector with height (Davenport 1987). Gradient wind speeds estimated from the NOAA surface data following this protocol were cross-referenced against the gradient extrapolations of surface winds from Midway and O'Hare (using the BLWTL wind climate model for Chicago) and were found to show good consistency.

Though wind-induced displacements are characterized by both background (quasistatic) and resonant components, only the latter can be recovered by the aforementioned accelerometer system. Therefore, it was of interest to monitor both of these contributions in full scale. Global positioning systems (GPS) could offer such capabilities and were added as secondary instrumentation, allowing dynamic displacements to be tracked with high accuracy (on the order of millimeters) at sampling rates of 10 Hz, while capturing the static and quasistatic displacements contributed by the background component of wind-induced response. A differential GPS sensor pair was installed on Building 1 and on a nearby stationary reference building on August 26, 2002. The choke-ring, GPS antenna, affixed to a rigid mount and topped by a protective radome (Fig. 1), was installed at the centerline on the penthouse rooftop of Building 1 to capture building sway along both axes. The GPS receiver, supporting electronics, and on-site laptop, which is remotely interrogated via modem to trigger the system and download data, are housed indoors in an enclosure nearby the data logger system discussed previously (Fig. 1). In this differential configuration, the Leica MC 500 sensors used in this study are capable of achieving a resolution, in terms of RMS background noise, of less than 5 mm, based on calibrations conducted before full-scale deployment (Kijewski-Correa 2003). In full scale, the predicted RMS resolution is estimated as 7.6 mm based on the baseline separation between Building 1 and the reference station. More details of GPS theory and the performance of the system used in this study can be found in Kijewski-Correa and Kareem (2003).

Analytical Modeling

The following sections discuss the wind tunnel testing of each of the buildings as performed by the BLWTL and the finite-element modeling of the buildings conducted by SOM.

Wind Tunnel Testing

The model-scale wind-induced responses of the three buildings selected for the study were measured in the high-speed section of the closed-circuit wind tunnel (BLWT II) at the BLWTL at UWO. The length of the high-speed section of the tunnel is approximately 38.5 m, and the dimensions of the tunnel at the test section are 4.5 m × 2.5 m (width by height). The top speed of the wind tunnel is approximately 27 m/s, measured at the entrance of the high-speed test section.

Though aeroelastic model tests would provide direct information on aerodynamic damping effects and, depending on the type of model, contributions of higher modes of vibration to the response, the high-frequency force-balance (HFFB) method was chosen for the wind tunnel tests as it allows the flexibility to repeat response predictions based on the measured modal force spectra but considering different building dynamic properties without the requirement of additional wind tunnel testing. Accordingly, differences between the in situ and predicted structural properties of the buildings are easily reconciled using the HFFB method as compared to aeroelastic tests.

The modeling for the force balance tests conducted in this study consisted of three components: (1) a rigid and lightweight detailed scale model of each of the study buildings; (2) a detailed model of the structures surrounding the building sites within a full-scale radius of about 750 m; and (3) a less detailed model of the upstream terrain, chosen to simulate the scaled turbulence intensity and velocity profiles expected at full scale for each site. The force balance model's geometry was replicated at a scale of 1:500 using very stiff, lightweight foam. The stiffness of each model was further augmented by the insertion of a tubular aluminum spine, which extends into the model approximately half the model height. The tubular spine was glued to the building shell,

Table 2. Terrain and Surface Roughness Lengths Assumed for Profile Development

Terrain description	Effective roughness length z_0 (m)
Water/lake	0.0022–0.0043[a]
Open	0.03
Suburbs/outskirts of city	0.3–0.5
Urban/city center	1.0–3.0

[a]Roughness length over water is estimated as a function of the local friction velocity (after ESDU 01008).

and the entire assembly was fixed to a rigid magnesium base plate. The building models were then rigidly attached to a six-component JR3 load cell.

Though all the buildings are located in downtown Chicago (Fig. 2) and are, generally speaking, sited in urban terrain, the mean wind velocity and the turbulence intensity profiles are expected to differ at each site. Thus, for each building, wind velocity and turbulence intensity profiles were modeled corresponding to three general terrain exposures: (1) an open exposure for winds approaching from Lake Michigan, with modifications to consider fetches of heavily built-up urban terrain along the lakeshore; (2) a suburban exposure modified to account for the heavily built-up urban downtown business district of Chicago; and (3) a suburban exposure for winds approaching from west through north wind directions, modified where appropriate to reflect the heavily built-up section of Chicago known as "The Magnificent Mile."

The velocity and turbulence intensity profiles used for the model scale tests of the three buildings in this study were based primarily on a categorization of the terrain surrounding the sites and the Engineering Sciences Data Units (ESDU). Three sources of information were used to categorize the terrain: (1) scaled aerial photographs of the sites available freely via the Internet (Terraserver 2004); (2) recommendations in Davenport et al. (2000) for the roughness lengths of various terrains; and (3) the ESDU 01008 Data Unit (ESDU 2001). The roughness length values and the associated terrains assumed in the profile development are provided in Table 2. Typical velocity and turbulence profiles developed during the wind tunnel studies are presented in Fig. 3.

A generalized view of a typical wind tunnel test configuration is shown in Fig. 4. In this study, each building was tested at 10° increments for the full 360° azimuth range. Time histories of the responses, as well as the mean and RMS base bending and torsional moments, were recorded and their associated power spectra were subsequently obtained. The generalized forces acting on the building in the sway directions are related to the base moments through approximately linear mode shapes $\phi(z)$, written as

$$\phi(z) = a\left(\frac{z}{H}\right) \tag{1}$$

where z=height above grade; H=height of the structure; and a=constant. The relation between the generalized force in the torsional mode and the base torque measured by the balance is not analogous to the sway directions. An empirical correction to the measured base moment is applied to correct the estimate of the generalized force (a typical correction factor of 0.7 is applied at the BLWTL). The generalized force in mode j at each time increment is evaluated as follows:

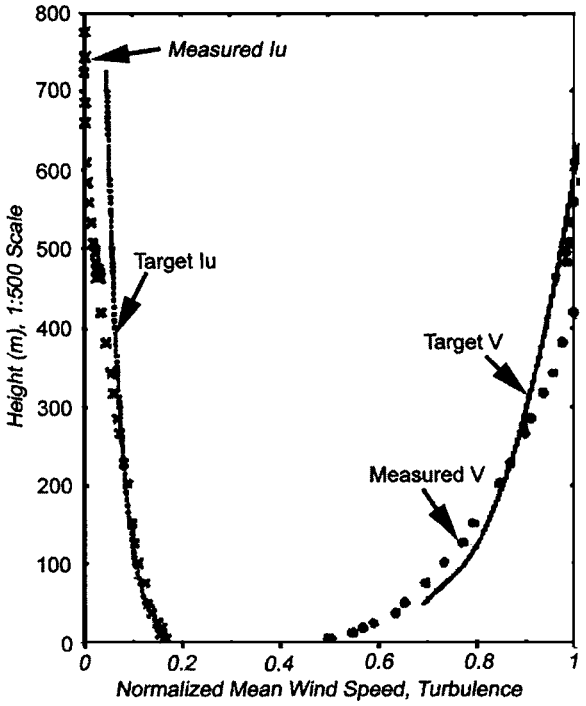

Fig. 3. Simulated mean wind speed (●) and turbulence intensity (×) profiles with solid and dashed lines indicating target profiles, respectively

$$F_j^*(t) = \int_0^H f_x(z,t)\phi_{xj}(z)dz + \int_0^H f_y(z,t)\phi_{yj}(z)dz + \int_0^H f_\theta(z,t)\phi_{\theta j}(z)dz \tag{2}$$

where

$$\int_0^H f_x(z,t)\phi_{xj}(z)dz \approx \int_0^H f_x(z,t)a_{xj}\left(\frac{z}{H}\right)dz = \frac{a_{xj}}{H}M_x(t) \tag{3a}$$

$$\int_0^H f_y(z,t)\phi_{yj}(z)dz \approx \int_0^H f_y(z,t)a_{yj}\left(\frac{z}{H}\right)dz = \frac{a_{yj}}{H}M_y(t) \tag{3b}$$

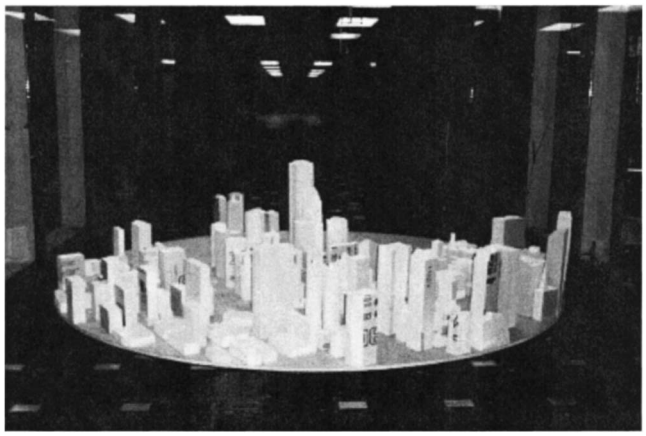

Fig. 4. Photo of typical proximity model for city of Chicago used in wind tunnel testing

$$\int_0^H f_\theta(z,t)\phi_{\theta j}(z)dz \approx 0.7a_{\theta j}T(t) \tag{3c}$$

where $M_x(t)$, $M_y(t)$, and $T(t)$=base moments in x, y, and torsion; and a_{xj}, a_{yj}, and a_{zj}=modal mixing factors. Note that corrections (Vickery et al. 1985) to adjust for nonlinear mode shapes are applied to obtain improved estimates of the generalized forces for prediction of accelerations. Additional mode shape correction procedures are given in Zhou et al. (2002) and include an assessment of the efficacy of the various techniques. Using the above formulations, the generalized force in mode j at each time increment can be written in terms of the measured base moments as

$$F_j^*(t) = \frac{a_{xj}}{H}C_{xj}M_x(t) + \frac{a_{yj}}{H}C_{yj}M_y(t) + 0.7a_{\theta j}C_{\theta j}T(t) \tag{4}$$

where C_{xj}, C_{yj}, and C_{zj}=mode shape corrections. In the HFFB method, the responses of the buildings are typically described by the dynamic responses in the first three fundamental modes of vibration.

The resulting RMS acceleration along the building's x axis at any height z_{acc} above grade due to the generalized force acting in mode j may be written as follows:

$$\sigma_{\ddot{x}_j} = (2\pi f_j)^2 \frac{\sigma_{F_j^*}^2}{K_j^*}\phi_{xj}(z_{acc})\sqrt{\frac{\pi}{4\zeta_j}\frac{f_j S_{F_j^*}(f_j)}{\sigma_{F_j^*}^2}} \tag{5}$$

where f_j=natural frequency in mode j; $\sigma_{F_j^*}^2$=variance of the generalized force in mode j; K_j^*=generalized stiffness in mode j; $S_{F_j^*}(f_j)$=value of the power spectral density of the generalized force at the natural frequency; and ζ_j=structural damping in mode j. Accelerations in the y axis and torsional directions are similarly defined. The maximum acceleration in the x direction is comprised of the components acting in modes $j=1,\ldots,3$, which are combined using the complete quadratic combination (CQC) method as follows:

$$\sigma_{\ddot{x}} = \sqrt{\sum_i \sum_j \sigma_{\ddot{x}_i}\rho_{ij}\sigma_{\ddot{x}_j}} \tag{6}$$

where $\sigma_{\ddot{x}_i}$ and $\sigma_{\ddot{x}_j}$=modal accelerations in the x axis in modes i and j; and ρ_{ij}=modal cross-correlation coefficient. For well separated frequencies, the cross-correlation coefficient ρ_{ij} approaches 0, and the total acceleration in the x direction may be written simply as the sum of the root-sum of squares (SRSS) of the acceleration components in Modes 1–3.

More advanced modal combination procedures have recently been proposed in Chen and Kareem (2004, 2005), which are particularly valuable for buildings with closely spaced frequencies. Under these conditions, the modal cross-correlation coefficient depends not only on the modal frequencies and damping ratios, but also on the correlation/coherence of the attendant generalized forces. This important consideration for accurate utilization of the CQC scheme has neither been fully recognized in the literature nor in current wind tunnel practice. Any implication of this recent development on the results of this study will be reported in the near future. However, due to the rather modest level of coupling, the results may not be significantly affected when compared to other sources of uncertainty, e.g., estimates of gradient wind speeds from surface level winds.

Finite-Element Modeling

Throughout the design stages, structural engineers rely on finite-element (FE) models to predict the full-scale behavior of buildings. Such aspects as overall damping, translational and torsional frequencies, and the associated mode shapes define the dynamic characteristics of the structure. These fundamental characteristics are used in wind tunnel testing to predict equivalent static wind loads that are then applied to the building model for the survivability level design of components and are also used in the analysis procedure outlined in the preceding section to predict accelerations that are used to assess the acceptability of the building motions in terms of occupant comfort. For tall, slender buildings and those lightly damped, motion perception often becomes the governing design criteria. Therefore, it is critical that the engineer be able to accurately predict the full-scale behavior of the structure by means of analytical representation through a FE model. For the buildings associated with this study, finite-element models were developed using currently available commercial software: ETABS (ETABS 2002) and SAP 2000 (SAP 2002), based upon careful reference to the design drawings. It was not the purpose of this study to apply a unique set of modeling assumptions to the FE models in order to mimic a known, in situ measured result. Rather, all assumptions regarding the FE representation of the buildings in this study reflect those commonly applied in design offices for serviceability assessment.

In order to predict the modal characteristics of the study buildings, an eigenanalysis was performed. The mass associated with the self-weight of the structure and the full weight of the exterior cladding system are included in the dynamic analysis. Additionally, special attention is paid to the use of the building and the resulting loading conditions at each floor in order to determine what fraction of the design imposed load to include in the mass calculations for the dynamic analysis. Due to the heights of the study buildings, the analysis includes the effects of building displacement on the frequencies through an elastic second-order (P-Δ) iteration. The buildings were modeled as fixed at the base, such that no base rotation exists. This is thought to approximate the generally high soil–structure interfacial stiffness observed in Chicago for buildings under transient lateral loads.

For Buildings 1 and 3, framed primarily in structural steel, the representation of the member stiffness was straightforward, as the steel elements are thought to remain elastic at service level loadings. For the reinforced concrete building (Building 2), adjustments were made to selected lateral-load resisting elements to represent the postcracking stiffness of these elements under service level loads. Specifically, the flexural and shearing stiffnesses of the link (coupling) beams within the shear wall system were reduced to one half and one fifth of the elastic stiffness, respectively. The beam-supported slab, was modeled using shell elements. The flexural stiffness of the slab's shell elements was set to one half of the elastic stiffness in order to approximate the postcracking behavior of the slab, which transfers flexure and shear between the perimeter columns and core shear walls. While generally considered to support gravity floor loads alone, explicit modeling of the linkage between the floors, exterior columns, and core often results in a substantial contribution to lateral resistance in reinforced concrete buildings. It should be noted that while modern finite-element computer analysis models account for the actual mass and stiffness distribution throughout the structure, it is believed that lumped-mass models utilized at the time of the original design of Buildings 1–3 correlate well with the more detailed distributed mass models used in this study.

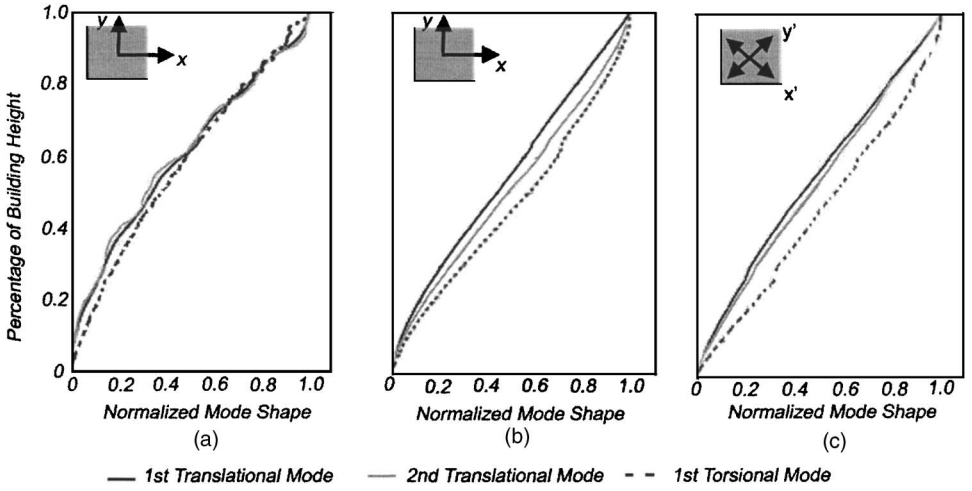

Fig. 5. Normalized fundamental mode shapes for Buildings (a) 1, (b) 2, and (c) 3

Fig. 5 shows the mode shapes for each of the buildings, normalized with respect to the top floor displacement. The inset in each figure shows the axes of vibration displayed in the plot. Table 3 summarizes the resulting periods from the FE analyses conducted at SOM and the damping levels assumed by the original designers of the buildings. Buildings 2 and 3 undergo coupled responses, though the extent of coupling in Building 2 is much less than Building 3. Note that although the writers acknowledge that Building 2 can be reasonably expected to have higher damping, the damping values of 1% for habitability/serviceability and 1.5% for survivability reported in Table 3 were the values specified in their design.

Web-Based Data Transmission and Processing

Possibly the greatest challenge in long-term monitoring projects is the transfer, processing, dissemination, and management of collected data, in particular for geographically dispersed collaborators. In this program, the data loggers are remotely interrogated by phone in a multihop configuration, using a communications hub at SOM (Kijewski et al. 2003). This information is then uploaded to an Apache 2.0.44 web server (Apache 2004), called "windycity," for access by the geographically dispersed project team (Kwon 2003). A Hypertext preprocessor (PHP) 4.3.1 (PHP 2004), a kind of Common Gateway Interface (CGI), is utilized to create interactive displays allowing users to select any record available for a given building. An alternative mode of data access is provided via structured query language (SQL), enabling a database query using MySQL (MySQL 2004) to identify records with a desired level of wind velocity or response resulting in an automatically updated listing of the available files satisfying these criteria [Fig. 6(a)]. Upon selecting a record, the data are postprocessed on-the-fly via MATLAB (MATLAB 2000) on the server side, with JAVA SDK 1.41-01 and JAVA Webstart 1.2 (Sun 2004) providing the interfacing capabilities. Through this process, described in Kijewski et al. (2003), any spikes and drifts are removed to preserve data quality, voltages are converted to engineering units and responses at the corners of the building are decoupled to extract the sway and torsional accelerations in a computationally efficient manner [Fig. 6(b)].

Data Inventory

A total of over 8,000 h of time histories have been collected thus far in the program. During this monitoring period, numerous wind events have been observed with mean hourly wind speeds exceeding 18 m/s, many associated with the windiest spring on record for the city of Chicago since 1991. During March and April of 2004, 11 "damaging wind speed" events were recorded (Wachowski 2004). Two particularly noteworthy events were those on March 5, 2004 and April 28, 2004. The former caused damage to building in downtown Chicago and was compared to a "mild hurricane" (Janega and Munson 2004), while the latter event spanned 2 days and is the subject of analysis in subsequent

Table 3. Periods of Vibration and Assumed Damping Levels for Finite-Element Models of Buildings 1–3

Building	Mode 1		Mode 2		Mode 3	
	Period	Damping	Period	Damping	Period	Damping
1	*Y* axis translation		*X* axis translation		Torsion	
	7.0 s	1%	4.9 s	1%	2.0 s	1%
2	*X* axis translation slight torsion		*Y* axis translation, slight torsion		Coupled torsion	
	6.7 s	1%[a]	6.4 s	1%[a]	4.6 s	1%[a]
3	Fully coupled *x* translation		Fully coupled *y* translation		Fully coupled torsion	
	7.7 s	1%	7.6 s	1%	4.5 s	1%

[a]1% used for accelerations, 1.5% used for base moments.

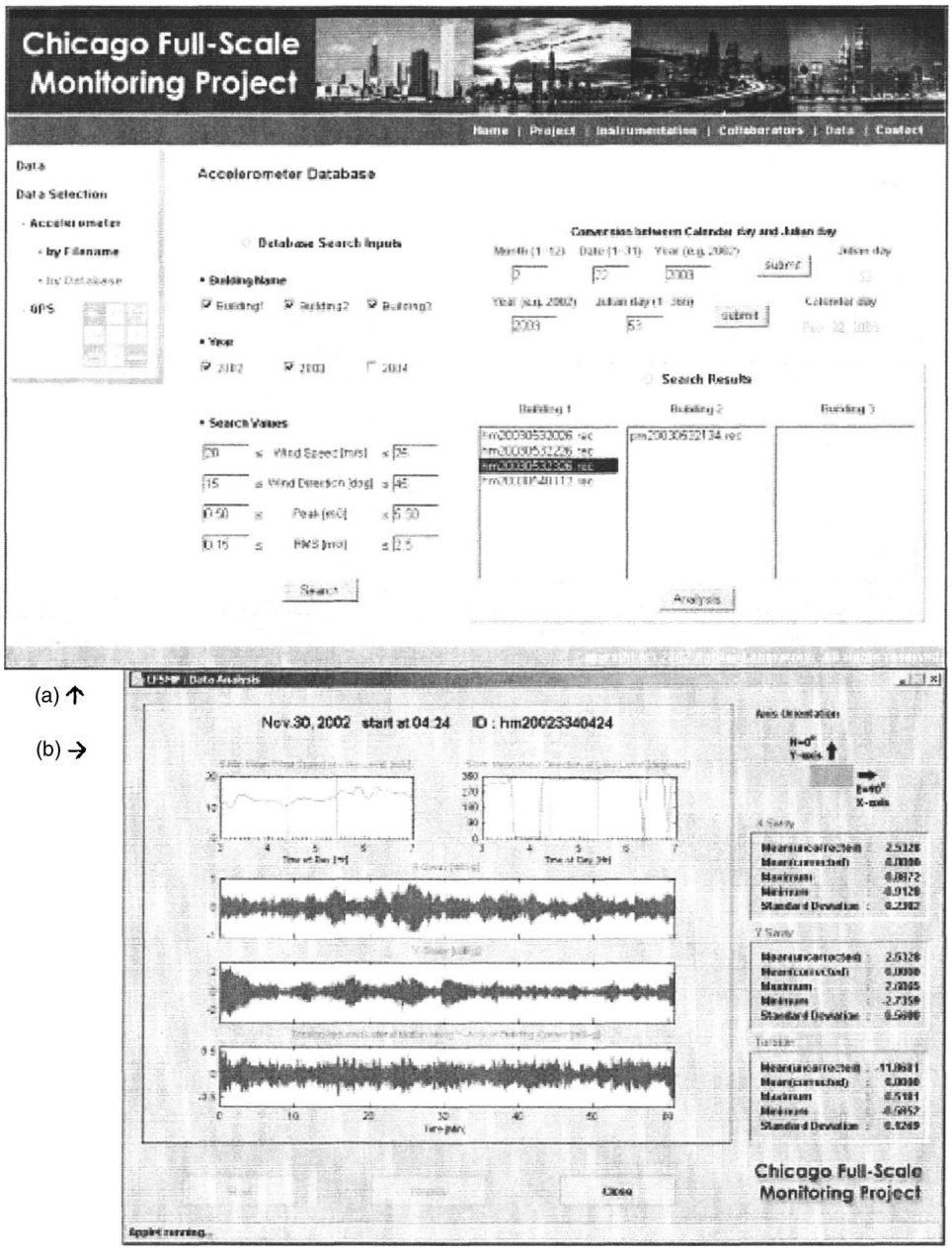

Fig. 6. (a) User interface for database query; (b) JAVA enabled data display

sections of this paper. In addition, two seismic events were recorded. The first event, on June 18, 2002, was a magnitude 5.0 event near Evansville, Ind., modestly exciting the *N-S* axis of Building 1. The second event, on June 28, 2004, was a magnitude 4.5 event near Ottawa, Ill., which caused some minor excitation of Building 2.

Example Response Analysis

While an extensive comparison of predicted and measured responses and a catalog of measured dynamic properties and their amplitude dependence are presented in companion papers by the writers, an example of the measured response of all three buildings for the April 28–29, 2004 wind event is now presented. A second data sampling for Building 1 during the February 11, 2003 wind event was presented in Kilpatrick et al. (2003).

Discussion of Wind Field and Response Characteristics

For the following discussion, wind field characteristics are described by the output of the NOAA GLERL sensor. As this sensor samples wind speed and direction every 5 s and records 5 min averages, the wind velocity recordings were reaveraged over 1 h periods to yield mean hourly wind speeds [Fig. 7(a)]. These results are then extrapolated to gradient level by two methods. Method 1 involves the use of power law expressions, coefficients and gradient heights readily available in ASCE 7-02 (ASCE 2003), assuming that winds approaching the lakefront sensor from the city are consistent with Exposure C, while associating winds approaching from open waters of Lake Michigan with Exposure D. This result is shown in Fig. 7(b). Method 2, shown in Fig. 7(c), uses the interim wind protocol discussed previously in the "Instrumentation Overview" section. The surface level wind direc-

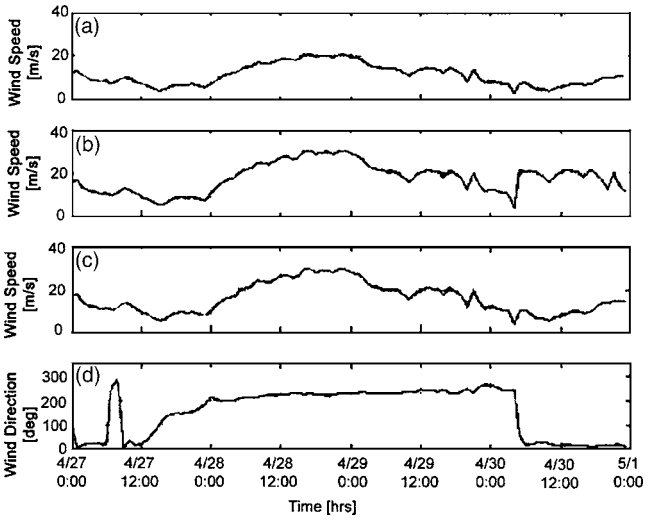

Fig. 7. (a) NOAA GLERL surface level mean hourly wind speed; (b) gradient level mean hourly wind speed translated by Method 1; (c) gradient level mean hourly wind speed translated by Method 2; and (d) NOAA GLERL surface level wind direction

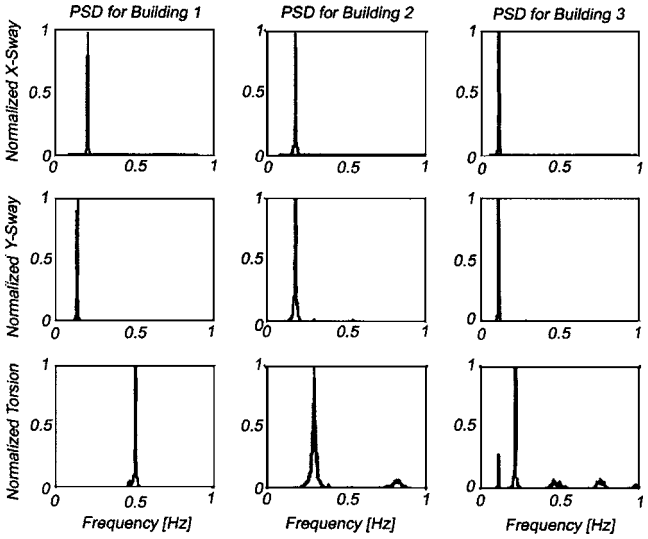

Fig. 8. Matrix of power spectral densities of acceleration response in x, y, and torsion for Buildings 1–3 in April 28, 2004 wind event

tions are provided in Fig. 7(d). A comparison of Figs. 7(b and c) demonstrates a good agreement between methods conventionally used by commercial wind tunnel testing facilities [Method 2, Fig. 7(c)] and those standardized in ASCE 7 [Method 1, Fig. 7(b)]. The intensification of the storm over April 28th culminates with several hours of mean hourly gradient winds consistently in the vicinity of 30 m/s, then steadily diminishing on the 29th. This "steady" wind period will be used for identification of dynamic properties in the next section.

Extracted Dynamic Properties

To determine the natural frequency and damping of the three buildings under ambient vibrations, two system identification (SI) techniques assuming stationary white noise inputs were utilized, a power spectral approach using the half-power band width (HPBW) technique (Bendat and Piersol 1986) and the random decrement technique (RDT) (Cole 1973; Kareem and Gurley 1996). The reliability of these two approaches for system identification from ambient vibrations has been evaluated by Kijewski and Kareem (2002). Both approaches invoke assumptions of stationarity, which cannot be fully validated for the wind on-site, as anemometer measurements are not available at all of the buildings in the program. However, stationarity can be established for the acceleration responses of each building for the April 28–29 wind event, using a variety of stationarity tests. These tests included the run and reverse arrangements tests (Bendat and Piersol 1986) and a more practical stationarity check proposed by Montpelier (1996). As shown in Fig. 7, wind speed and direction stabilized between approximately 2:00 and 10:00 p.m. on April 28, 2004. The application of the three stationarity tests to the candidate records within this time period revealed that very few records passed the run test, but almost all records passed at least one of the other two tests, with several passing both. In some cases, stationarity could be achieved in all three response directions for a given record. It was determined that passing at least two of the stationarity tests was sufficient, leading to the following respective success rates for each of the buildings: 95.2, 77.8, and 91.7%. Only records satisfying these conditions were used in the aforementioned time and frequency domain system identification analyses.

Spectral Analysis

Given the narrowbanded nature of the buildings in this study, the simultaneous reduction of bias and variance errors can be quite challenging, given the limited amount of data satisfying the stationarity checks conducted here. In light of this, spectral damping is generally overestimated and can have significant uncertainty in light of variance errors. Nevertheless, the identified stationary data were broken into segments of sufficient length so as to provide a minimum of four spectral lines in the half power bandwidth, a condition necessary for bias errors of less than −2% (Bendat and Piersol 1986). Given the frequencies of the buildings, the segment length varied from 4,096 to 16,384 and produced 12–53 segments that were processed by the fast Fourier transform (FFT), squared and averaged to produce the power spectra shown in Fig. 8. From these spectra, a few details are evident. Naturally the narrowband feature of the buildings and the dominance of fundamental mode are expected, with minor participation by the higher modes. Recall that the wind during this event approaches from the west–southwest. Also note evidence of coupling in Buildings 2 and 3. Though minor in the former, algebraic manipulations of the channel outputs could not totally isolate the torsional response from the sway in Building 3. From these spectra, dynamic properties are extracted by the HPBW approach from all significant modes, though only fundamental mode estimates are provided here for brevity.

Random Decrement Technique

The stationary response data were first preprocessed by Butterworth bandpass filters to isolate each mode of interest before applying the RDT. The decrement signatures were then generated by capturing a sample of prescribed length from the filtered time history that satisfies the trigger condition X_p. The segments initiating with this trigger are averaged to essentially remove the random component of the response, leaving random decrement

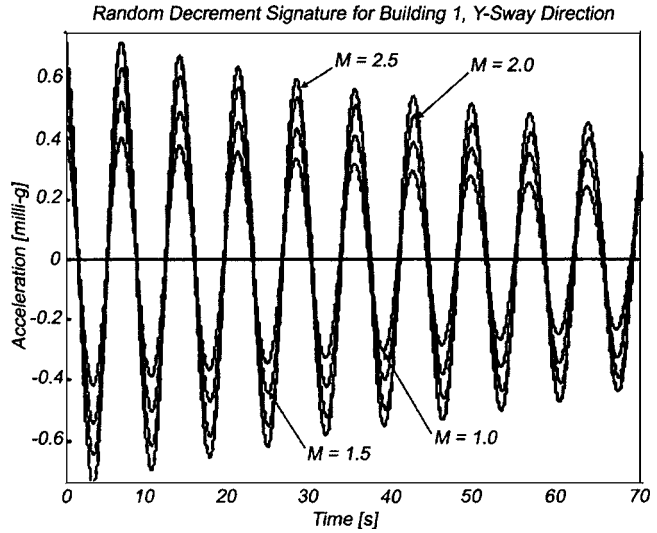

Fig. 9. Suite of RDS using multiple trigger approach for Building 1, *y*-sway response in April 28, 2004 wind event

signature (RDS). This expectation operation was shown by Vandiver et al. (1982) to produce an RDS proportional to the autocorrelation signature $[R_{xx}(\tau)]$ for the system

$$D(\tau) \equiv E[X(t_2)|X(t_1) = X_p] = X_p R_{xx}(\tau)/R_{xx}(0) \quad (7)$$

The expectation in Eq. (7), assuming ergodicity, can be replaced by an average of the triggered segments taken from a single time history. Given the assumptions of Gaussian, zero mean, white noise driving a linear system, the autocorrelation function takes a form proportional to the decay curve

$$R_{xx}(\tau) \propto e^{-\zeta\omega_n\tau}\cos(\omega_D\tau) \quad (8)$$

where ω_n=natural frequency (rad/s); and ω_D=damped natural frequency (rad/s).

Thus once the RDS is obtained, it is fit using a standard Hilbert transform approach (Bendat and Piersol 1986) to extract frequency and damping from the phase and amplitude of the analytic signal, though a wavelet-based approach may also be used, eliminating the need for the aforementioned bandpass filtering (Kijewski and Kareem 2003). Due to the sensitivity of trigger conditions on the number of segments captured, thereby impacting the variance of the RDS, the reliability of the RDT can be improved through repeated triggering, as proposed in Kijewski-Correa (2003). This is accomplished by generating RDSs for positive point triggers that are multiples of the standard deviation of the acceleration response being analyzed ($X_p=M\sigma$). By using a range of triggers, multiple stable decrement signatures can be obtained and analyzed to produce a range of estimates of natural frequency and damping, as demonstrated in Fig. 9. The damping and frequency associated with each trigger can be studied to reveal any amplitude dependence of the dynamic properties (Jeary 1992; Tamura and Suganuma 1996), or the values can be averaged to give an estimate of frequency and damping comparable to that of a spectral-based approach. Furthermore, an estimate of the variability in the approach, quantified through a coefficient of variation (COV) of these results from this suite of RDSs, provides a much needed reliability measure (Kijewski and Kareem 2002). In this example, given the limited amount of data considered, the RDS suite will be used in the latter form to supply an averaged estimate of frequency and damping, accompanied by a COV estimate. The study of amplitude dependence will be addressed separately in a future publication where larger data sets are considered.

Table 4. Periods of Vibration Estimated by Spectral and Time Domain Analyses for April 28, 2004 Wind Event

		Building 1	Building 2	Building 3
HPBW	*x*-sway	4.89	5.62	8.60
	y-sway	7.06	5.65	8.62
	Torsion	1.99	3.41	4.48
RDT	*x*-sway	4.89	5.61	8.60
	(COV)	(0.10%)	(0.22%)	(0.25%)
	y-sway	7.11	5.66	8.60
	(COV)	(0.19%)	(0.68%)	(0.14%)
	Torsion	1.99	3.41	4.35
	(COV)	(0.07%)	(0.71%)	(0.14%)

Discussion

The period and damping estimates by the aforementioned spectral and time-domain approaches are, respectively, presented in Tables 4 and 5. These are compared to the design predictions shown previously in Table 3. For reference, the relative responses of *x* sway, *y* sway, and torsion-induced lateral sway during this event were: 1:1.7:0.17 for Building 1, 1:0.52:0.05 for Building 2, and 1:0.76:0.12 for Building 3. This confirms the lack of torsional response in the buildings, as expected. Further, the behaviors of Buildings 2 and 3 show the amplified response in the *E-W* direction (*x* sway), characteristic of a dominant across-wind response for this wind event. This is not the case in Building 1, however, where the across-wind axis (*x* sway) is considerably stiffer (see Table 3), yielding a dominant along-wind response for this wind event.

Generally, excellent consistency between the two approaches is observed for period estimation. The exception is the torsional mode of Building 3, which still manifested evidence of coupling (Fig. 8) and thus difficult to filter and analyze by the RDT approach. The COV for all the RDT analyses are well under 1%, demonstrating the reliability with which periods are identified. In Building 1, periods of vibration show excellent agreement between the predictions in Table 3 and the in situ values. Some

Table 5. Damping (as Percent Critical) Estimated by Spectral and Time Domain Analyses for April 28, 2004 Wind Event

		Building 1	Building 2	Building 3
HPBW	*x*-sway (%)	0.65	1.62	**1.46**
		(*N*=26)	(*N*=33)	(***N*=12**)
	y-sway (%)	**1.14**	2.07	**1.06**
		(***N*=13**)	(*N*=33)	(***N*=12**)
	Torsion (%)	0.74	3.14	1.31
		(*N*=53)	(*N*=33)	(*N*=24)
RDT	*x*-sway (%)	0.87	1.42	1.04
	(COV) (%)	(23.9)	(7.4)	(20.6)
	y-sway (%)	0.88	2.4	1.21
	(COV) (%)	(8.9)	(8.0)	(23.0)
	Torsion (%)	0.87	3.59	1.33
	(COV) (%)	(14.9)	(13.4)	(16.9)

Note: *N* indicates number of raw spectra in PSD average. Values shown in bold correspond to analyses with higher variance error.

slight discrepancy is noted between the HPBW and RDT result for *Y* sway, which being a very long period response, provides fewer averages in both the spectral and RDT methods, as evidenced by its relatively higher COV. Building 2 demonstrates periods 11–25% stiffer in situ than predicted by the FE models. This may be attributed to the FE model's stiffness reductions due to cracking that has yet to be observed in the service life of this building. It is equally possible that the in situ modulus of elasticity is larger than that assumed in the FE modeling. Building 3, on the other hand, has in situ periods that are generally longer than FE model predictions, by approximately 10%. Further investigation of this building's response has also revealed amplitude dependence in its sway periods. The roles of panel zone stiffness, service condition mass variability, foundation stiffness, and beam/column frame connectivity were explored by the writers in a recent publication (Kijewski-Correa et al. 2005) in an effort to understand more completely these in situ behaviors.

As expected, the COV of damping estimates by RDT are markedly higher than those of period estimates, reaffirming the difficulty in estimating damping. In addition to the COV, the number of raw spectra averaged in the power spectral estimates is provided in Table 5 to give an indication of the variance errors. Again bias was first minimized to under −2%, but this leaves potentially high variance errors for a limited amount of data. This is particularly relevant to the spectral damping estimates for the longer period responses (Building 1 *y* axis and Building 3 *x* and *y* axes). For example, analyses of Building 1 presented in Kilpatrick et al. (2003) utilize 20 h of data (more than twice the amount here). Despite its reduced duration, the April 28–29, 2004 was of noteworthy intensity and therefore interest. However, the RDT results, which were generated from segments numbering in the thousands, likely provide a more reliable estimate of damping and showed consistency with the results in Kilpatrick et al. (2003) for Building 1. Recall that the relative levels of damping were speculated for each of the buildings in the "Description of Instrumented Buildings" section. This speculation indicated that Building 1 would have the least damping and Building 2 the most. This speculation has indeed been confirmed by the in situ damping levels in Table 5 for each response component, particularly in light of the RDT results. Given also that the return period of this event is approximately annual, and the assumed damping levels are intended for larger return periods, then the use of 1% damping in the design of these three buildings was likely appropriate for Building 1 and even conservative for Building 3, given the general assumption of amplitude dependence in damping (Jeary 1986). In the case of Building 2, the assumption of 1% seems highly conservative, as expected for a concrete structure.

Comparisons to Wind Tunnel Predictions

A comparison of full-scale accelerations from Buildings 1, 2, and 3 with wind tunnel predictions is now made for the April 28–29, 2004 wind event shown previously in Fig. 7. Torsional responses are not shown for brevity, since they are comparatively smaller. Note that at the design stage of a typical tall building, the inherent damping of a structure is rarely known with certainty, and estimates of the damping are made based on full-scale observations of similar structures. Given the potential variabilities in these and other critical parameters, upper and lower limits on predicted responses are presented here, based on the range of damping ratios that may be reasonably anticipated for each building given the COVs in Table 5, the frequencies of vibration observed in full scale, and the range of wind directions recorded during the event. This suite of values is summarized in Table 6.

Table 6. Range of Wind Directions, Fundamental Periods, and Damping Ratios Used in Wind Tunnel Predictions

Building	Wind direction (degrees)	*N-S* sway, period (s)	*E-W* sway, period (s)	*N-S* sway, damping (%)	*E-W* sway, damping (%)
1	230–250	7.10	4.90	0.7–1.0	0.7–1.0
2	230–250	5.66	5.61	1.5–2.0	1.0–1.5
3	230–250	8.60	8.60	1.25–1.5	1.0–1.25

The measured and predicted RMS responses of Buildings 1, 2 and 3 in the *E-W* and *N-S* direction are plotted against the estimated gradient wind speed in Figs. 10–12, respectively. A complication in the study to date has been the lack of reliable upper level wind speed measurements. Ideally, upper level wind speeds would be recorded simultaneously with the building responses through the data logger system. Though ultrasonic anemometers are located above the rooftop of Building 3, they were not in place for this wind event. Thus, the wind speed data utilized here are extrapolated from NOAA met station measurements in accordance with the interim wind monitoring protocol discussed in the "Instrumentation Overview" section. Also note that each building's RMS accelerations are normalized by the wind tunnel's predicted annual extreme acceleration for that particular response component, to assess the quality of the predictions while preserving anonymity of the buildings' response magnitudes as per the agreements with the building owners. The measured full-scale data in Figs. 10–12 correspond to the RMS accelerations recorded over 10-min intervals by the data logger system from approximately 6:00 p.m. on April 28 until 12:00 p.m. April 29 during which time the estimated gradient wind direction was relatively stable from the west–southwest. Note that the spread between upper and lower limits of response vary for each building and even each response direction due to the aerodynamic sensitivity of the particular building axis to wind direction and the inherent structural damping assumed in the analysis.

In Building 1, the wind tunnel predictions slightly underestimate *E-W* response, while overestimating *N-S* response. Agreement for Building 2 is generally very good and slightly conservative for the *N-S* response. Observed responses of Building 3 distribute rather uniformly about the predicted wind tunnel values. It is important to note that the NOAA wind speed and direction estimates are not necessarily representative of conditions at each building, potentially explaining some of the observed scatter about the wind tunnel predictions. Research into the comparisons of the full-scale and model-scale results for other wind events is ongoing to yield a more comprehensive assessment of analytical predictions in light of full-scale observations. Similar comparisons have been recently made for the displacements of Building 1 using the GPS sensor (Kochly and Kijewski-Correa 2005).

Comparison of Accelerometer and GPS Data

To date, in 49 significant wind events, GPS displacement data have also been recorded, providing over 300 h of data of full-scale displacement data. While more detailed discussion of GPS data in this program is provided in a companion paper (Kijewski-Correa et al. 2006), the effectiveness of GPS technology for full-scale dynamic monitoring is now demonstrated for this April 28,

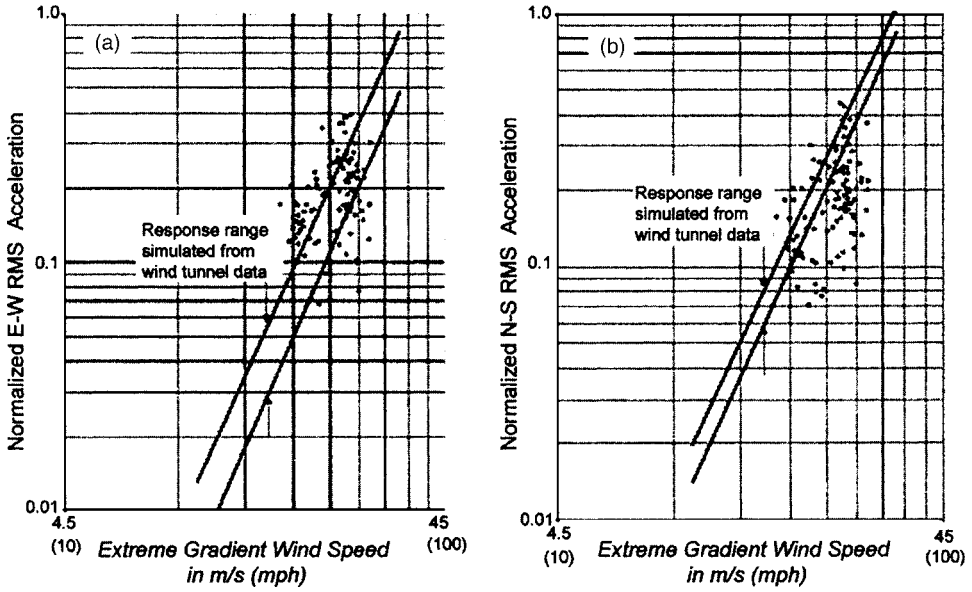

Fig. 10. Building 1—measured accelerations versus wind tunnel predictions for: (a) *E-W*; (b) *N-S* RMS sway response in April 28–29, 2004 wind event

2004 wind event. A double differencing method was used to convert the resonant GPS displacements to accelerations. These accelerations are compared to those measured during the event in Fig. 13 and show very good agreement. As demonstrated in Table 7, in terms of RMS measures, the two sensing techniques are within approximately 5% of each other. Given the harsh environment and interference levels associated with monitoring in urban environments, the good correlation between new sensing technologies like GPS and existing technologies like accelerometers is quite promising. Coupled with the continued investigation of urban multipath effects (Kijewski-Correa et al. 2004), this GPS unit in Chicago will allow the background component of wind-induced response to be observed in full scale and correlated against wind tunnel predictions for the first time, as demonstrated by the preliminary results in Kochly and Kijewski-Correa (2005).

Ongoing Activities and Extensions

At present, the writers continue to collect and analyze wind speed and response data from the three buildings in Chicago and intend to do so as long as owner cooperation and funding permit, providing a greater probability of recording significant wind events (5- or 10-year storms) associated with serviceability-level design. Recall that, to date, only annual wind events have been observed and only from select angles of attack. As a more diverse collection of noteworthy wind events is acquired, the writers will have the opportunity to conduct more detailed studies of in situ amplitude-dependent dynamic properties in both fundamental and higher modes and full-scale validations of wind tunnel predictive tools over a range of wind speeds and directions. This will allow the writers to make more definitive assessments of the accuracy

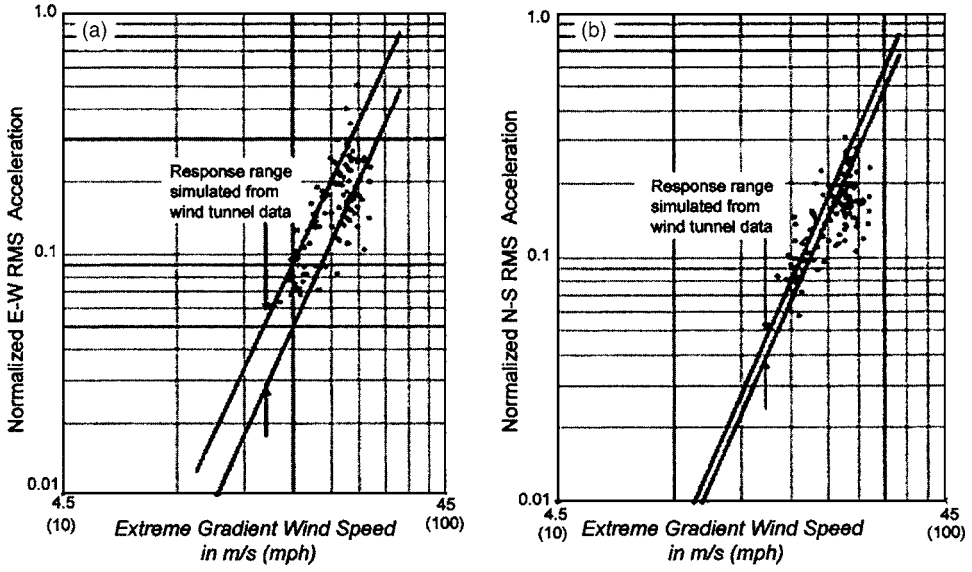

Fig. 11. Building 2—measured accelerations versus wind tunnel predictions for: (a) *E-W*; (b) *N-S* RMS sway response in April 28–29, 2004 wind event

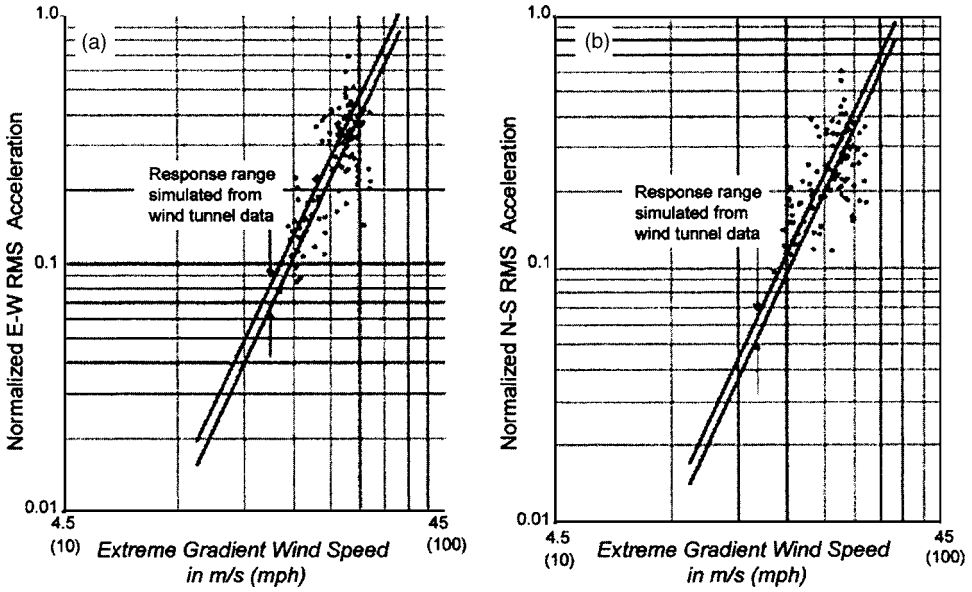

Fig. 12. Building 3—measured accelerations versus wind tunnel predictions for: (a) *E-W*; (b) *N-S* RMS sway response in April 28–29, 2004 wind event

of current design practices and make recommendations for improvement, if necessary. In particular, the effects of transient/nonstationary wind events on in situ response are being documented and techniques for identification of dynamic properties from such data are being developed. Finite-element analyses are also ongoing to explore the stiffness properties of Building 3, investigating in particular the influence of panel zone deformations on the overall behavior of the building.

While these efforts represent a first step toward developing a comprehensive full-scale validation of tall building design practice, the program could be greatly enhanced by an expansion of the instrumentation suite and buildings monitored. With regard to

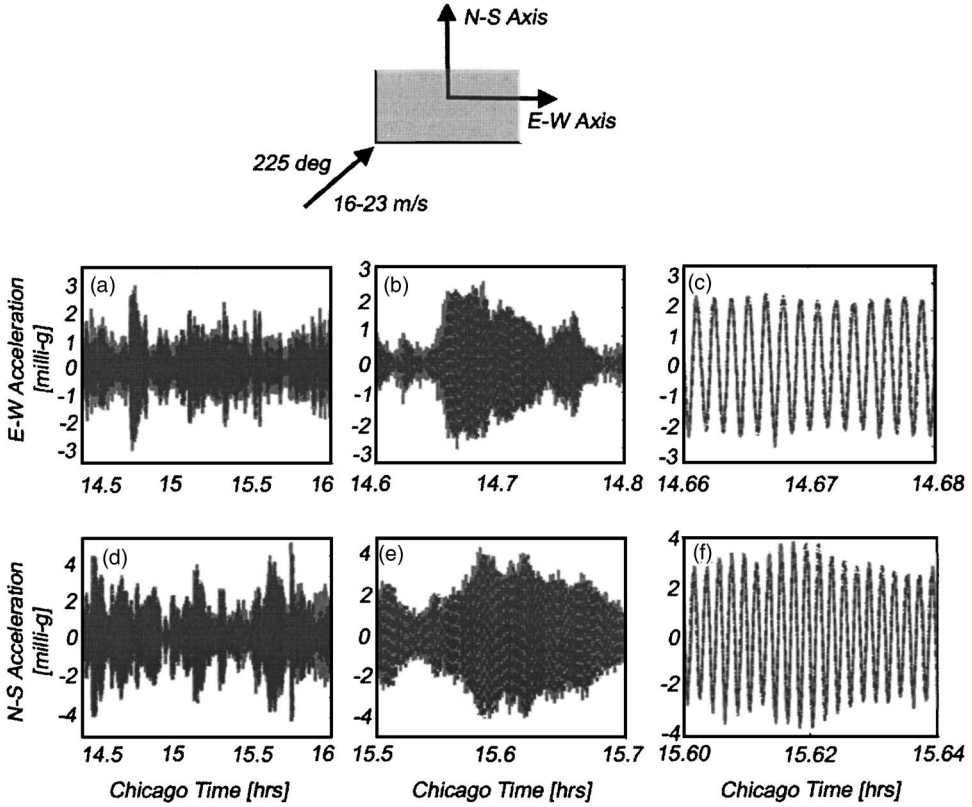

Fig. 13. Progressive zoom of accelerations by GPS (solid) plotted atop those by accelerometer (dashed) for April 28, 2004 wind event: (a)–(c) *E-W* motions and (d)–(f) *N-S* motions. Schematic of building axes and wind velocity vector at lake level shown above.

Table 7. Comparison of RMS Accelerations in Full Scale by Accelerometer and GPS

E-W		*N-S*	
Accelerometer	GPS	Accelerometer	GPS
0.61 milli-g	0.64 milli-g (+4.9%)	1.09 milli-g	1.15 milli-g (+5.5%)

the former, by placing anemometers at each of the monitored buildings, a more accurate description of the wind conditions on site could be obtained, allowing the wind field characteristics, including stationarity, to be investigated and calibrations of computational fluid dynamics models to be conducted. Deployments of GPS at each building would also allow more background response quantification, while the placement of accelerometers over the height of each building would provide in situ mode shape verification. With respect to expanding the suite of buildings being monitored, this would certainly strengthen any recommendations being made by the writers, given the variability of response characteristics and structural properties, particularly damping, with construction material, foundation type, and structural system. Such expansions are currently being pursued by the writers, subject to funding availability and owner consent.

Concluding Remarks

This paper introduces a study established to allow the first systematic validation of tall building performance in the United States using full-scale data in comparison with wind tunnel and finite-element models generally used in design. For each of the three tall buildings currently monitored in the city of Chicago, instrumentation is overviewed and wind tunnel and analytical modeling approaches are summarized. A comparison of the full-scale response features with design predictions is provided for the April 28–29, 2004 wind event. This comparison indicates that with respect to fundamental periods of vibration, standard modeling assumptions can reliably predict in situ periods of the uncoupled steel building. However, the assumptions made in the modeling of the reinforced concrete building in the study cannot be wholly validated, possibly due to levels of cracking assumed in the various service states not yet being realized in full scale as well as with the possibility that the in situ modulus of elasticity is higher than that assumed in the model. Reasons for the discrepancies and amplitude dependence in the sway periods for Building 3 may stem from a number of sources currently being investigated by the writers over a range of wind events.

With respect to damping, as a relatively short duration stationary period in this wind event was considered, sufficient data were not available to accurately resolve damping in all response directions of all buildings using spectral-based approaches. A potentially more reliable multiple trigger RDT approach applied to this annual wind event data did reveal that damping levels assumed at 1% for serviceability design were likely conservative for the concrete and even coupled steel buildings (Buildings 2 and 3), given the common presumption of amplitude dependence. The 1% damping assumption seems appropriate for the uncoupled steel building (Building 1). These damping estimates further support speculative opinions on the relative damping in each building, by virtue of their unique deformation mechanisms and construction materials. However, as this represents the conclusions based on the analysis of an isolated wind event, the appropriateness of these assumed damping levels will be more thoroughly verified with the continued analysis of data collected in the program.

Evaluations of the predicted accelerations from wind tunnel testing revealed that the full-scale data had a reasonable level of scatter but followed the general trend of the wind tunnel predictions. Finally, a comparison of traditional sensors used in the program (accelerometers) and new sensing technologies (GPS) was provided and demonstrates the potential of GPS to accurately track the motions of tall buildings under wind. As this research is ongoing, this paper is intended to chronicle the establishment of the program and the types of analyses being conducted on the full-scale response data.

Acknowledgments

The writers wish to gratefully acknowledge the support of the National Science Foundation through Grant No. CMS 00-85109, UND, BLWTL, SOM, the Chicago Committee on High Rise Buildings, and Canada's Natural Sciences and Engineering Research Council, which supported the second writer. The writers must also sincerely thank the building owners and management for their continued cooperation and enthusiasm, as well as students/engineers, technicians, legal counsel, and support staff at UND, BLWTL, and SOM for their efforts.

References

Apache Software Foundation. (2004). ⟨http://www.apache.org⟩ (July 15, 2004).

ASCE. (2003). "Minimum design loads for buildings and other structures." *SEI/ASCE 7-02*, Reston, Va.

Bendat, J. S., and Piersol, A. G. (1986). *Random data: Analysis and measurement procedures*, 2nd Ed., Wiley, New York.

Chen, X., and Kareem, A. (2004). "Coupled building response analysis using HFFB: Some new insights." *Proc., 5th Int. Colloquium on Bluff Body Aerodynamics and Applications*, Ottawa.

Chen, X., and Kareem, A. (2005). "Dynamic wind load effects on buildings with 3D coupled modes: Application of HFFB measurements," *J. Eng. Mech.*, 131(11), 1115–1125.

Cole, H. A. (1973). "On-line failure detection and damping measurement of aerospace structures by random decrement signatures." *NASA CR-2205*, NASA, Washington, D.C.

Davenport, A. G. (1987). "The structure of wind and climate." *The application of wind engineering principles to the design of structures*, Lausanne, Switzerland, 103–156.

Davenport, A. G., Grimmond, C. S. B., Oke, T. R., and Wieringa, J. (2000). "Estimating the roughness of cities and sheltered country." *Proc, 15th Conf. on Probability and Statistics in the Atmospheric Sciences/12th Conf. on Applied Climatology*, Asheville, N.C.

Denoon, R. O., Letchford, C. W., Kwok, K. C. S., and Morrison, D. L. (1999). "Field measurements of human reaction to wind-induced building motion." *Wind engineering into the 21st century*, A. Larsen, G. L. Larose and F. M. Livesey, eds., Balkema, Rotterdam, The Netherlands, 637–644.

Engineering Sciences Data Unit-01008 (ESDU). (2001). *Computer program for wind speeds and turbulence properties: Flat or hilly sites in terrain with roughness changes*, London.

ETABS. (2002). *ETABS version 8.0, reference manual*, Computer & Structures, Inc., Berkeley, Calif.

Janega, J., and Munson, N. (2004). "Blown for a loop: Winds grab bricks, hats and cash." *Chicago Tribune*, 6 March, 1.

Jeary, A. P. (1986). "Damping in tall buildings—A mechanism and a predictor." *Earthquake Eng. Struct. Dyn.*, 14, 733–750.

Jeary, A. P. (1992). "Establishing nonlinear damping characteristics of structures from non-stationary response time histories." *Struct. Eng.*, 70(4), 61–66.

Kareem, A., and Gurley, K. (1996) "Damping in structures: Its evaluation and treatment of uncertainty." *J. Wind. Eng. Ind. Aerodyn.*, 59(2,3), 131–157.

Kareem, A., Kijewski, T., and Tamura, Y. (1999). "Mitigation of motions of tall buildings with specific examples of recent applications." *Wind Struct.*, 2(3), 201–251.

Kijewski, T., and Kareem, A. (2002). "On the reliability of a class of system identification techniques: Insights from bootstrap theory." *Struct. Safety*, 24(2–4), 261–280.

Kijewski, T., and Kareem, A. (2003). "Wavelet transforms for system identification: Considerations for civil engineering applications." *Comput. Aided Civ. Infrastruct. Eng.*, 18, 341–357.

Kijewski, T., Kwon, D. K., and Kareem, A. (2003). "E-technologies for wind effects on structures," *Proc, 11th Int. Conf. on Wind Engineering* (CD-ROM), Texas Tech Univ., Lubbock, Tex.

Kijewski-Correa, T. (2003). "Time-frequency perspectives in system identification: From theory to full-scale measurement." Ph.D. dissertation, Univ. Notre Dame, Notre Dame, Ind.

Kijewski-Correa, T., and Kareem, A. (2003). "The height of precision." *GPS World*, 14(9), 20–34.

Kijewski-Correa, T., Kochly, M., and Stowell, J. (2004). "On the emerging role of GPS in structural health monitoring." *Proc., CTBUH 2004*, CTBUH, Chicago, 144–151.

Kijewski-Correa, T., Young, B., Baker, W. F., Sinn, R., Abdelrazaq, A., Isyumov, N., and Kareem, A. (2005). "Full-scale validation of finite element models for tall buildings." *Proc., CTBUH 2005* (CD-ROM), CTBUH, Chicago.

Kijewski-Correa, T., Kareem, A., and Kochly, M. (2006). "Experimental verification and full-scale deployment of global positioning systems to monitor the dynamic response of tall buildings." *J. Struct. Eng.*, 132(8), 1242–1253.

Kilpatrick, J., et al. (2003). "Full scale validation of the predicted response of tall buildings: preliminary results of the Chicago monitoring project." *Proc, 11th Int. Conf. on Wind Engineering* (CD-ROM), Texas Tech Univ., Lubbock, Tex.

Kochly, M., and Kijewski-Correa, T. (2005). "Monitoring tall buildings under the action of wind: The role of GPS in urban zones." *Proc., 4th European & African Conf. on Wind Engineering* (CD-ROM), ITAM, Prague, Czech Republic.

Kwon, D. K. (2003). "Chicago full-scale monitoring program." ⟨http://windycity.ce.nd.edu⟩ (November 15, 2003).

Li., Q. S., Fang, J. Q., Jeary, A. P., and Wong, C. K. (1998). "Full scale measurements of wind effects on tall buildings." *J. Wind. Eng. Ind. Aerodyn.*, 74–76, 741–750.

Li, Q. S., Xiao, Y. Q., Wong, C. K., and Jeary, A. P. (2004). "Field measurements of typhoon effects on a super tall building." *Eng. Struct.*, 26, 233–244.

Li, Q. S., Yang, K., Zhang, N., Wong, C.-K., and Jeary, A. (2002). "Field measurements of amplitude-dependent damping in a 79-storey tall building and its effects on structural dynamic responses." *Struct. Des. Tall Build.*, 11, 129–153.

Littler, J. D. (1991). "The response of a tall building to wind loading." Ph.D. dissertation, Univ. of London, London.

MATLAB. (2000). *Using MATLAB, version 6 (release 12)*, The MathWorks, Inc., Natick, Mass.

Montpelier, P. R. (1996). "The maximum likelihood method of estimating dynamic properties structures." Master's thesis, Univ. of Western Ontario, Ontario, Canada.

MySQL AB. (2004). *MySQL*, ⟨http://www.mysql.com⟩ (July 15, 2004).

Ohkuma, T. (1996). "Japanese experience with motions of tall buildings." *Rep. to Council on Tall Buildings in Urban Habitat (CTBUH) Committee 36: Motion Perception and Tolerance*, Lehigh, Pa.

Ohkuma, T., Marukawa, H., Niihori, Y., and Kato, N. (1991). "Full-scale measurement of wind pressures and response accelerations of a high-rise building." *J. Wind. Eng. Ind. Aerodyn.*, 38, 185–186.

PHP. (2004). *Hypertext preprocessor*, ⟨http://www.php.net⟩ (July 15, 2004).

SAP. (2002). *SAP 2002 version 8.0, reference manual*, Computer & Structures, Inc., Berkeley, Calif.

Satake, N., Suda, K., Arakawa, T., Sasaki, A., and Tamura, Y. (2003). "Damping evaluation using full-scale data of buildings in Japan." *J. Struct. Eng.*, 129(4), 470–477.

Sun Microsystems, Inc. (2004). *The source for Java technology*, ⟨http://java.sun.com⟩ (July 15, 2004).

Tamura, Y., and Suganuma, S.-Y. (1996). "Evaluation of amplitude-dependent damping and natural frequency of buildings during strong winds." *J. Wind. Eng. Ind. Aerodyn.*, 59(2,3), 115–130.

Terraserver. (2004). ⟨http://terraserver.homeadvisor.msn.com/⟩ (July 1, 2004).

Vandiver, J. K., Dunwoody, A. B., Campbell, R. B., and Cook, M. F. (1982). "A mathematical basis for random decrement vibration signature analysis technique." *J. Mech. Des.*, 104, 307–313.

Vickery, P. J., Steckley, A., Isyumov, N., and Vickery, B. J. (1985). "The effect of mode shape on the wind-induced response of tall buildings." *Proc., 5th United States National Conf. on Wind Engineering*, Texas Tech Univ., Lubbock, Tex.

Wachowski, F. (2004). "Windiest spring since 1991: Powerful wind gusts." *Chicago Tribune*, 2 May.

Zhou, Y., Kareem, A., and Gu, M. (2002). "Mode shape corrections for wind load effects." *J. Eng. Mech.*, 128(1), 15–23.